



## Article

# Development of Bilayer Polysaccharide-Based Films Combining Extrusion and Electrospinning for Active Food Packaging

Rodrigo F. Gouvêa and Cristina T. Andrade \*

Programa de Pós-Graduação em Ciência de Alimentos, Instituto de Química, Universidade Federal do Rio de Janeiro, Avenida Moniz Aragão 360, Bloco 8G/CT2, Rio de Janeiro 21941-594, RJ, Brazil; rfgouvea@pos.iq.ufrj.br

\* Correspondence: ctandrade@iq.ufrj.br

**Abstract:** The development of active food packaging is desirable for food safety and to avoid food loss and waste. In this work, we developed antioxidant bilayer films combining extrusion and electrospinning techniques. These films consisted of a first layer of thermoplastic cornstarch (TPS), incorporated with microcrystalline cellulose (MCC). The second layer consisted of gallic acid (GA) encapsulated at different concentrations in 1:1 chitosan/poly(ethylene-co-vinyl alcohol) (CS/EVOH) nanofibers. This layer was directly electrospun onto the TPS/MCC film. The morphological, structural, wettability, permeability to oxygen, and antioxidant properties were investigated for the first layer and the bilayer films. Water contact angle measurements revealed the hydrophobic nature of the first layer ( $\theta_0 = 100.6^\circ$ ). The oxygen permeability (OP) was accessed through the peroxide value (PV) of canola oil, kept in containers covered by the films. PV varied from 66.6 meq/kg for the TPS/MCC layer to 60.5 meq/kg for a bilayer film. Intermolecular hydrogen bonds, mediated by GA, contributed slightly to improving the mechanical strength of the bilayer films. The bilayer film incorporated with GA at 15.0% reached a radical scavenging activity against the DPPH radical of  $(903.8 \pm 62.2) \mu\text{mol.L}^{-1}.\text{Eq. Trolox.g}^{-1}$ . This result proved the effectiveness of the GA nanoencapsulation strategy.

**Keywords:** thermoplastic starch; chitosan; bilayer films; extrusion; electrospinning; antioxidant films



**Citation:** Gouvêa, R.F.; Andrade, C.T.

Development of Bilayer Polysaccharide-Based Films Combining Extrusion and Electrospinning for Active Food Packaging. *Polysaccharides* **2024**, *5*, 129–141. <https://doi.org/10.3390/polysaccharides5020010>

Academic Editor: Ioannis S. Chronakis

Received: 24 March 2024

Revised: 6 May 2024

Accepted: 7 May 2024

Published: 9 May 2024



**Copyright:** © 2024 by the authors. Licensee MDPI, Basel, Switzerland. This article is an open access article distributed under the terms and conditions of the Creative Commons Attribution (CC BY) license (<https://creativecommons.org/licenses/by/4.0/>).

## 1. Introduction

Food loss and waste have received special attention from international organizations, researchers, and the food industry. Several strategies have been proposed to confront this issue. The use of appropriate food packaging was appointed as one of the strategies to reduce food loss and waste [1,2]. Active food packaging prolongs the shelf life of food products by inhibiting damage caused by microbial, enzymatic, and oxidative attacks [3].

To inhibit oxidative reactions, antioxidants have been incorporated directly into food. This procedure is justified by the potential effectiveness of antioxidants in scavenging reactive species. Gallic acid (GA, 3,4,5-trihydroxybenzoic acid) is an example of a natural substance with antioxidant, anticancer, anti-inflammatory, and antimicrobial properties. GA is found in fruits, vegetables, and herbs [4]. However, the unpleasant taste of gallic acid prevents its use directly in food [5]. Moreover, GA is sensitive to basic pH, high temperatures, oxygen, and light [6]. To overcome these drawbacks, encapsulation methods are recommended to protect bioactive substances and control the rate of their release. Electrohydrodynamic techniques (electrospinning and electrospraying) may be cited as relatively simple and nonthermal methods of encapsulation [7]. By these methods, bioactive substances are incorporated into nanofibers and nanoparticles without losing their activity [8,9]. The large surface area-to-volume ratio of nanofibers and the high porosity of membranes are desirable to tune the release of bioactive substances from the packaging material to the food product [10]. Recently, GA was encapsulated in hydroxypropyl methylcellulose/poly(ethylene oxide) electrospun nanofibers to produce an active packaging material [5].

Bearing in mind that food packages are generally used only once before disposal and that synthetic polymer waste is responsible for environmental and health concerns, alternative biobased materials represent a sustainable and attractive alternative [11,12]. Starch, cellulose, and chitosan are among the main biopolymers used for this purpose [12]. Cellulose is the most abundant polysaccharide on earth. Cellulose and starch are formed of D-glucose-repeating units. These constituting D-glucose units are linked by  $\beta$ -1,4 and  $\alpha$ -1,4 glycoside bonds in cellulose and starch, respectively. This difference defines cellulose as a structural polymer and starch as a reserve material. Chitosan is generally obtained by the deacetylation of chitin, which is mainly found in the exoskeleton of crustaceans. Chitosan is composed of  $\beta$ -(1,4)-2-amino-2-deoxy-D-glucose and  $\beta$ -(1,4)-2-acetamido-2-deoxy-D-glucose repeating units. However, polysaccharides present high hydrophilicity. This property, associated with their mechanical and thermal properties, limits their applications in food packaging when used alone. These disadvantages are minimized by the development of biocomposites [13] and bi- or multilayer films [14,15].

The objective of this work was to combine two techniques, extrusion and electrospinning, to prepare bilayer films aimed at extending the shelf life of foods. For the first layer, thermoplastic starch (TPS) was prepared by extrusion with the addition of microcrystalline cellulose (MCC) at 2.0 mass% content. The second layer consisted of chitosan-based electrospun nanofibers, collected on the TPS/MCC layer. GA was loaded into the second layer. However, in aqueous solutions, the electrospinning of chitosan (CS) alone is a difficult process because of its high molar mass and polycationic nature [16]. Because of this difficulty, GA was incorporated into a CS/poly(ethylene-co-vinyl alcohol) (EVOH) mixed solution. A high oxygen barrier, thermal resistance, and good optical properties favor the extensive use of EVOH in food packaging [17]. The bilayer films were characterized for their morphological, structural, thermal stability, wettability, permeability to oxygen, mechanical, and antioxidant properties.

## 2. Materials and Methods

### 2.1. Materials

Regular cornstarch (RS), constituted of 74–70 mass% amylopectin and 26–30 mass% amylose, with 12% humidity, was donated by Ingredion Brasil Ingredientes Industriais Ltd.a. (São Paulo, SP, Brazil). CS, MCC, GA and 2,2-diphenyl-1-picrylhydrazyl (DPPH) were purchased from Sigma–Aldrich Brasil Ltda. (São Paulo, SP, Brazil). The degree of deacetylation (DD = 85%) and the viscosity-average molar mass ( $\overline{M}_v \sim 296,700$ ) of the CS sample were previously reported [18]. EVOH from Gantrade Corporation (Montvale, NJ, USA) was characterized by HPDEC-MAS NMR at 10 kHz in a Bruker Avance III 400 MHz (Bruker Corporation, Billerica, MA, USA). The ethylene and vinyl alcohol compositions were determined to be 44.29% and 55.71%, respectively. Canola oil (rapeseed oil) was purchased from a local market. All other materials were purchased from Isofar Indústria e Comércio de Produtos Químicos (Rio de Janeiro, RJ, Brazil).

### 2.2. Preparation of TPS/MCC Layer

MCC (6 g) was mixed manually with glycerol (90 g) in a mortar for 30 min. Granular RS (300 g) was homogenized with MCC/glycerol in a conventional mixer (Ika Works, Wilmington, NC, USA). The resulting mixture was extruded in a Coperion ZSK 18 (Werner & Pfleiderer, Stuttgart, Germany) co-rotating twin-screw extruder with a L/D ratio of 40. Its heating zones were kept at 110 °C–120 °C, and the screw speed was set at 200 rpm. After extrusion, the material was pelletized and compression-molded into films by heating at 135 °C under 68.9 MPa for 10 min, and cooling in a cold press for 5 min. The resulting films were designated as TPS/MCC and were kept in polyethylene bags under ambient conditions.

### 2.3. Preparation of Solutions for Electrospinning

A CS solution at 10 g/L was prepared in 1% acetic acid by stirring at room temperature for 18 h. The EVOH solution at 6% (*m/v*) was prepared in 70% isopropyl alcohol/water under reflux for 2 h [19]. GA was added at 5.0, 10.0, and 15.0% concentrations (*m/m*, based on the CS mass) and dispersed in CS solutions using a Ultra-Turrax (IkaWorks, Wilmington, NC, USA) at 5000 rpm for 1 h. CS/EVOH mixed solution at 1:1 composition and CS/EVOH solutions incorporated with GA were also prepared by stirring at ambient temperature for 10 min.

### 2.4. Electrospinning

Electrospinning was carried out using Hsensor Equipamentos Materiais e Acessórios Ltda. (Maringá, PR, Brazil) equipment, consisting of a syringe pump, a variable high-voltage (0–26 kV) DC power supply, and a stainless-steel plate as a collector. Preliminary experiments, varying CS:EVOH composition and other parameters, were performed to choose the best conditions for electrospinning the CS/EVOH solution. The chosen conditions were CS/EVOH at 1:1 composition, 15 kV (positive output voltage), 20 cm as the distance between the collector and the needle tip, and a flux of 0.66 mL/h. The solution was loaded into a 10 mL syringe and pumped through needles 0.5 mm in internal diameter onto the metallic collector, previously wrapped in aluminum foil. The temperature was maintained at 23 °C, and the relative humidity was 60%. CS/EVOH/GA solutions were electrospun onto the TPS/MCC film under the same conditions. Then, the materials were kept at ambient conditions for solvent evaporation. In the text and figures, the resulting bilayer films were named SM (bilayer film without GA) and SM5, SM10 and SM15 (bilayer films with GA added at 5.0, 10.0, and 15.0% concentrations).

### 2.5. Characterization of Materials

#### 2.5.1. Morphological Characterization

Cryogenically fractured surfaces of the films were imaged by SEM with a Vega 3LMU from Tescan Analytics (Brno-Kohoutovice, Czech Republic) microscope at an acceleration voltage of 5 kV. Surface images from electrospun layers were also analyzed. Prior to imaging, the samples were coated with gold.

#### 2.5.2. Structural Characterization by Fourier Transform Infrared Spectroscopy (FTIR)

The TPS/MCC composite film and the bilayer films were characterized at ambient temperature by FTIR with Nicolet iS50 equipment from Thermo Fisher Scientific (Madison, WI, USA), equipped with a Universal Attenuated Total Reflectance (ATR) cell device, in the 4000  $\text{cm}^{-1}$  to 600  $\text{cm}^{-1}$  range, by averaging 64 scans with a resolution of 4  $\text{cm}^{-1}$  in transmission mode. Other samples (CS, EVOH, and CS/EVOH) were characterized as KBr disks.

#### 2.5.3. Thermal Stability Characterization

The thermal stability of TPS/MCC and the bilayer films were investigated by thermogravimetric analyses (TGA) with a TGA Q-500 equipment from TA Instruments (New Castle, DE, USA). The samples were heated from 30 °C to 700 °C, at 10 °C/min under nitrogen atmosphere.

#### 2.5.4. Wettability

Sample wettability was characterized by measuring water contact angles (WCA). The experiments were performed by the sessile drop method, using a Ramé-Hart model 100 goniometer (Ramé-Hart Inc., Cedar Knolls, NJ, USA). A 2  $\mu\text{L}$  drop of distilled water was placed on the TPS/MCC surface of the films using an auto-pipette. A CCD video camera captured the image of the droplet, and the WCA was calculated with the Drop-Image software. The evolution of the droplet contact angle was registered during 300 s; six

measurements per second were taken. This procedure was carried out in triplicate, and the average values were considered.

#### 2.5.5. Oxygen Permeability

The oxygen permeability (OP) of the films was accessed through the peroxide value, determined according to the methodology reported elsewhere [20,21]. Samples of canola oil (10 mL) were kept in 25 mL bottles, covered with bilayer films, and fixed with common glue. For the control sample, the bottle was uncovered. The systems were kept at 60 °C for seven days [20,21]. Then, oil peroxidation was measured by titration with sodium thiosulfate, after adding a saturated solution of potassium iodide [21,22].

#### 2.5.6. Mechanical Properties

Thickness was measured at five different points of the samples with a Digimatic Caliper 500-144 model (Mitutoyo Sul Americana Ltd.a., Suzano, SP, Brazil). Tensile tests were performed to analyze the mechanical properties of the materials according to the ISO 527-3 method [23]. Rectangular specimens of the bilayer films with (18.0 ± 0.2) mm in length and (8.0 ± 0.1) mm in width were analyzed in a Q-800 DMA apparatus from TA Instruments at ambient temperature (21 °C). The experiments were carried out with a ramp force of 1.5 N/min to 18.0 N/min. The average value from at least three measurements was considered.

#### 2.5.7. Characterization of Antioxidant Activity

The free radical scavenging activity was determined by the DPPH method. The extraction of GA from the bilayer films was performed in 95% ethanol [24]. For the extraction step, the sample specimens (2.0 cm × 2.0 cm) were kept in the dark at ambient temperature in a tube with 4 mL of the ethanolic solution for 1 h, 3 h, and 24 h. For the antioxidant tests, aliquots of 0.1 mL of each extract or the Trolox standard solution (0 to 1.2 µM concentrations) were reacted with 3.9 mL of DPPH solution (0.1 mM). After 30 min in the dark, the absorbance was measured at 517 nm in the UV-vis spectrophotometer, UV-2600 model (Shimadzu Corporation, Kyoto, Japan) and compared to the Trolox calibration curve to determine the radical scavenging activity. The DPPH tests were performed in triplicate, and the results were expressed as µmol/L<sup>-1</sup> Trolox equivalent/g dry mass of film. The scavenging activity (AA%) was also determined according to the following equation.

$$AA\% = \frac{A_c - A_s}{A_c} \times 100$$

where  $A_c$  and  $A_s$  are, respectively, the absorbance of the DPPH solution and the absorbance of the samples submitted to the DPPH assay.

### 2.6. Statistical Analysis

The Statistica® v.8 software, associated with the one-way analysis of variance (ANOVA), was used to better analyze some data. Results were given as mean ± standard deviation. A  $p$ -value equal to or less than 0.05 was considered significant. Average values were compared using the Fisher's test.

## 3. Results and Discussion

### 3.1. Morphological Characterization

Figure 1 shows SEM images for the cross-sections of TPS/MCC and SM bilayer films. MCC particles of varying dimensions may be seen within the TPS composite layer. Most MCC particles appear stretched, revealing adhesion between the cellulose particles and the thermoplastic starch matrix (Figure 1a). A compact film was formed by electrospinning the 1:1 pure CS/EVOH mixed solution onto the TPS/MCC layer (Figure 1b). Differences in texture allow for distinguishing the interface between the layers (Figure 1b). In contrast, a porous layer was deposited on TPS/MCC when GA was added to the CS/EVOH mixture

(Figure 1c–e). In Figure 1e, obtained for the cross-section of SM15, the electrospun layer seems to be thinner than the others, probably as a result of increasing intermolecular interactions mediated by GA added at 15.0% concentration. The occurrence of intermolecular hydrogen bonds was expected because of the structural features of GA, CS, and EVOH, all of which have hydroxylic groups in their structures. CS also has amine groups, capable of forming hydrogen bonds with GA. The formation of intermolecular interactions between CS and GA was also suggested by other authors [25].

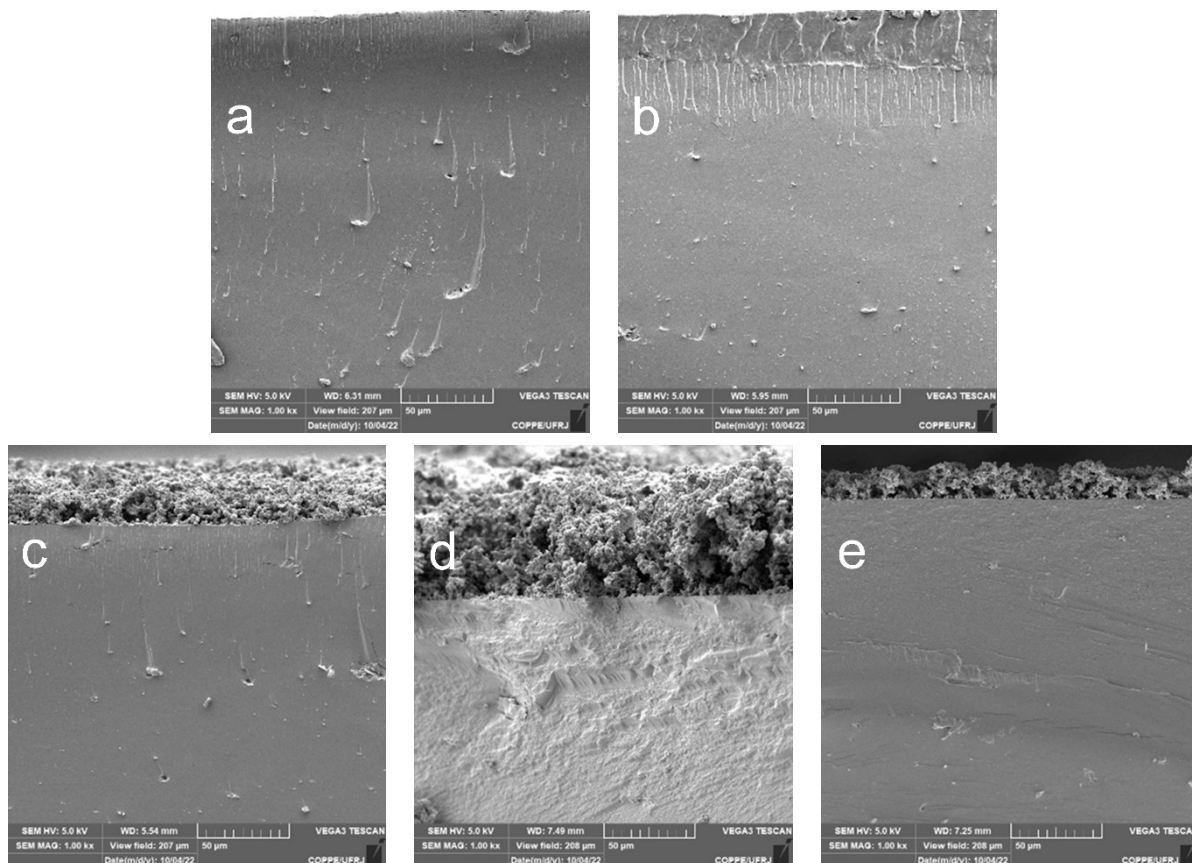


**Figure 1.** Scanning electron microscopy (SEM) images for the cross section of the TPS/MCC first layer (a) and bilayer films formed by CS/EVOH/GA electrospun onto TPS/MCC with the addition of GA at 0% (b), 5.0% (c), 10.0% (d) and 15.0% (e) concentrations. TPS: thermoplastic starch; MCC: microcrystalline cellulose; CS: chitosan; EVOH: poly(ethylene-co-vinyl alcohol); GA: gallic acid.

Figure 2 shows SEM images taken from the surfaces of the electrospun materials. The nanofibers produced from the EVOH solution (Figure 2a) were oriented randomly and presented an average diameter of  $416.4 \pm 89.9$  nm. Electrospinning the EVOH/CS mixed solution onto aluminum foil led to beaded nanofibers (Figure 2b), similar to that previously reported for CS alone [26]. However, when the EVOH/CS solution was electrospun onto TPS/MCC extruded film, without or with the addition of GA, aggregated and interconnected structures were visualized, forming a porous layer (Figure 2c–f). Similar morphologies were observed for CS/poly(ethylene oxide) electrospun nanofibers prepared from acetic acid solutions at various compositions [27].

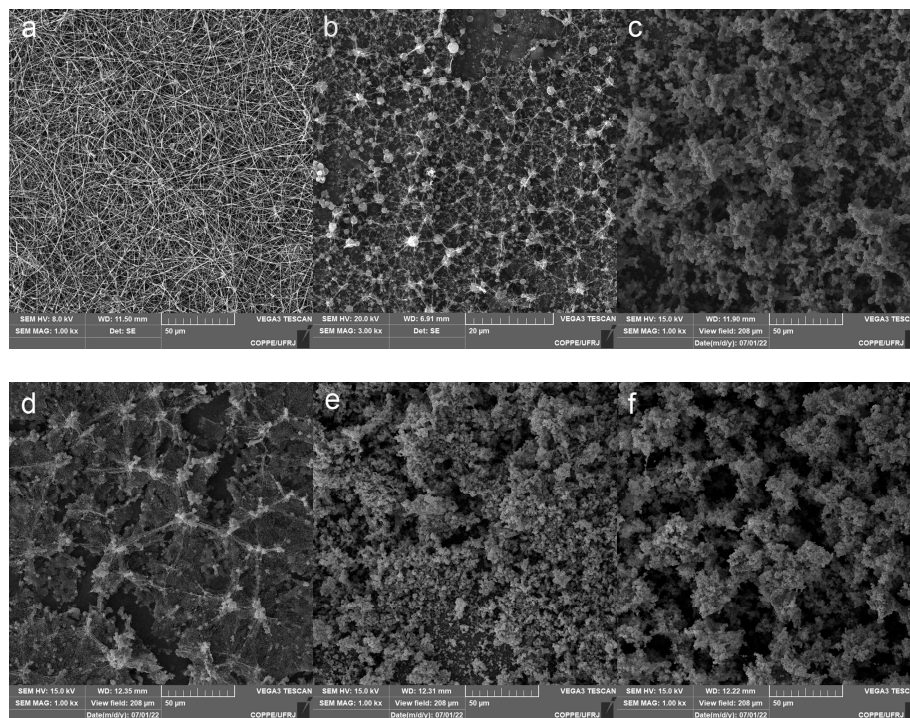


**Figure 2.** SEM micrographs for the surfaces of electrospun EVOH solution (a), electrospun CS/EVOH solution onto aluminum foil (b), electrospun CS/EVOH solution onto the TPS/MCC film without GA ((c), SM), and with the addition of GA at 5.0% ((d), SM5) 10% ((e), SM10) and 15% ((f), SM15). TPS: thermoplastic starch; MCC: microcrystalline cellulose; CS: chitosan; EVOH: poly(ethylene-co-vinyl alcohol); GA: gallic acid.

### 3.2. Structural Characterization by FTIR

Figure 3 shows the FTIR spectra for the first layer (TPS/MCC) and bilayer films. Figure S1 shows the spectra for CS and EVOH as powders and for the CS/EVOH nanofibers electrospun onto aluminum foil. In Figure 3, the broad absorption band observed for the polymeric components (starch, cellulose, CS, and EVOH) in the  $3600\text{ cm}^{-1}$ – $3000\text{ cm}^{-1}$  region is attributed to O–H stretching vibrations as well as to N–H stretching vibrations, in the case of CS [28]. For the TPS/MCC first layer and the SM bilayer film, this band has its maximum at  $3281\text{ cm}^{-1}$ . Adding GA to the EVOH/CS solution, this absorption maximum is shifted to higher wavenumbers for the films, as the GA concentration is increased. The C–H asymmetrical stretching vibration band, which appears at  $2926\text{ cm}^{-1}$  for TPS/MCC, is also shifted slightly to higher wavenumbers in the spectra for the bilayer films. Other authors attributed the band around  $1650\text{ cm}^{-1}$  to O–H bending from absorbed water [29]. This band also appears in all spectra. Probably, this band comprises the CS amide I band (Figure S1), attributed to C=O stretching vibrations of the amide groups [30]. For the bilayer films, the CS amide II band (Figure S1, at  $1592\text{ cm}^{-1}$ ), assigned to C–N stretching and C–N–H bending vibrations, is very weak. The band attributed to C–O–C stretching vibrations, which is observed at  $996\text{ cm}^{-1}$  for TPS/MCC, appears at  $1038\text{ cm}^{-1}$  for the SM bilayer film. With the incorporation of GA, this band shifts to higher wavelengths as the GA concentration increases. This result, associated with the shift of the O–H band, evidences the formation of hydrogen bonds between the components of the bilayer films, as previously suggested by a SEM image (Figure 1e). The existence of interactions between CS and GA was previously suggested by other authors [25], also following FTIR results.

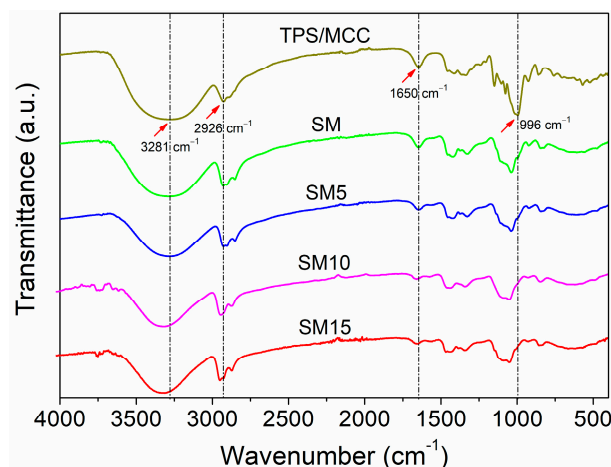


**Figure 3.** FTIR spectra for the TPS/MCC composite and bilayer films formed by electrospun CS/EVOH/GA onto TPS/MCC with the addition of GA at 0% (SM), 5.0% (SM5), 10.0% (SM10) and 15.0% (SM15) concentrations. TPS: thermoplastic starch; MCC: microcrystalline cellulose; CS: chitosan; EVOH: poly(ethylene-*co*-vinyl alcohol); GA: gallic acid.

### 3.3. Thermal Stability Characterization

Thermal stability is considered an important property for all materials. Thus, it was investigated for the first layer (TPS/MCC) and for the bilayer films by thermogravimetric analyses. In this case, it would be interesting to evaluate the effect of the electrospun layer on the thermal stability of the SM bilayer films. TG and DTG curves are depicted in Figure 4 and present similar profiles. Three stages of thermal degradation were observed. The first (~15%), related to the volatilization of free and bound water, which occurred up to ~186 °C and is frequently reported for other hydrophilic films [31,32]. For TPS/MCC, the second stage of thermal degradation (~175 °C–240 °C) is attributed to the thermal degradation of glycerol. The third stage is associated with the degradation of polymer molecules (starch and MCC). The onset of this thermal event begins at  $T_0 \sim 250$  °C, and the temperature of maximum degradation is at  $T_{max} = 317$  °C. In some other systems,  $T_{max}$  for starch was reported to occur around 300 °C [32–34]. This result may indicate the positive effect of MCC on the composite's thermal stability. For the bilayer films, the onset temperature of the third stage decreases slightly. In contrast,  $T_{max}$  slightly varied for the bilayer films (314 °C–316 °C). No improvement in thermal stability was observed by adding the electrospun layer to the TPS/MCC layer. The low molar mass GA, added to the electrospun layer as the active component, interacts with the polymeric components (CS and EVOH). GA degrades at a lower temperature than the polymers and, thus, has some influence on the degradation of the polymeric components [35].

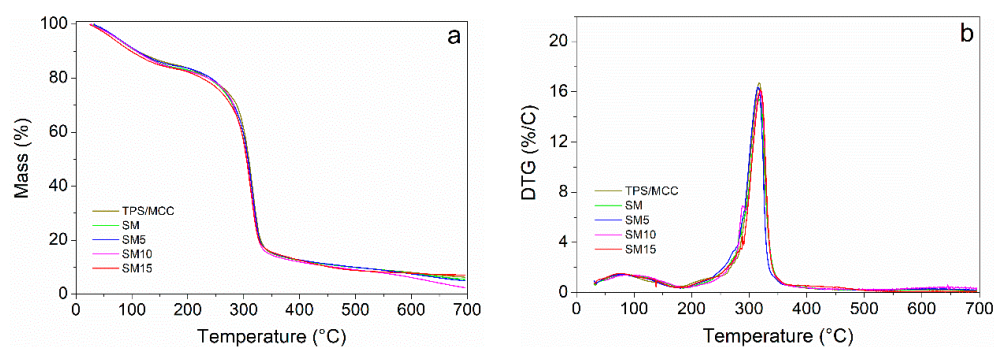


**Figure 4.** Thermogravimetric (a) and derivative thermogravimetric (DTG, (b)) curves for the first layer, thermoplastic starch incorporated with microcrystalline cellulose (TPS/MCC), and for the CS/EVOH bilayer films (SM) with the addition of GA at 0% (SM), 5.0% (SM5), 10.0% (SM10) and 15.0% (SM15) concentrations. CS: chitosan; EVOH: poly(ethylene-*co*-vinyl alcohol); GA: gallic acid.

### 3.4. Wettability

The surface wettability of the TPS/MCC and SM films was evaluated by measuring WCA (Figure 5). Figure 5a shows images of water drops registered at  $t_0$  (immediately after droplet deposition). Differences can be noticed in the images for the studied samples and allow for the classification of the materials according to the generally accepted relationship between contact angle and their hydrophilicity/hydrophobicity character [36,37]. The initial contact angle ( $\theta_0$ ) observed for the first layer, TPS/MCC, was  $\theta_0 = 100.6^\circ$ . It is important to point out that this result may be considered a high value for a starch-based material and characterizes the TPS/MCC surface as hydrophobic. Additionally, this result may be attributed to the water barrier property exerted by the MCC particles. In a previously published work, we found a much lower value for the initial water contact angle ( $\theta_0 = 43.4^\circ$ ) of extruded cornstarch plasticized with 25% glycerol [38]. Recently, MCC was prepared from elephant grass and added to cornstarch cast films at 1.0, 2.5, and 5.0% mass contents. The initial water contact angles varied from  $33.26^\circ$  to  $98.8^\circ$  [39]. While corroborating with the effect of MCC on WCA, the comparison with the result from this work suggests a better dispersion of MCC within the starch matrix by extrusion.

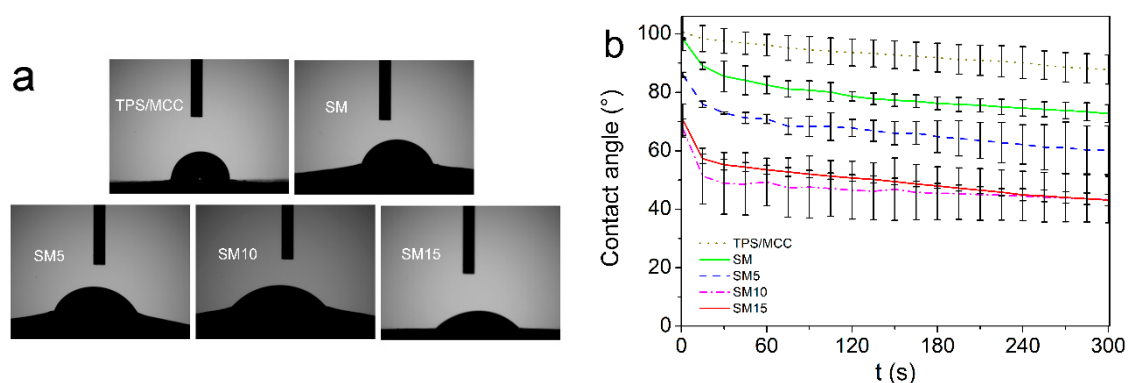


**Figure 5.** Water contact angle data: (a) Images for the water drop captured at the beginning of the experiment; (b) evolution of the contact angle on the TPS/MCC surface and on the TPS/MCC surface of the bilayer films formed by electrospun CS/EVOH/GA solutions onto TPS/MCC with the addition of GA at 0% (SM), 5.0% (SM5), 10.0% (SM10), and 15.0% (SM15) concentrations. TPS: thermoplastic starch; MCC: microcrystalline cellulose; CS: chitosan; EVOH: poly(ethylene-co-vinyl alcohol); GA: gallic acid.

A slightly lower  $\theta_0 = 98.3^\circ$  was determined for SM. This behavior indicates that the hydrophobic nature of the surface is maintained after the electrospinning of the CS/EVOH solution ( $90^\circ < \theta_0 < 150^\circ$ ) [36,37]. In contrast, the addition of GA to the CS/EVOH electrospun layer at 5.0, 10.0, and 15.0 mass% led to lower  $\theta_0$  values ( $\theta_0 = 86.0^\circ$ ,  $71.0^\circ$ , and  $68.0^\circ$  for SM5, SM10, and SM15 films, respectively). This result indicates that the encapsulation of the hydrophilic GA influences the water droplet absorption and wettability of the bilayer films. These films may be classified as hydrophilic ( $\theta_0 < 90^\circ$ ) [36,37]. This distinction among the samples may also be visualized as differences in droplet width in the images obtained at the beginning of the experiments (Figure 5a). A similar reduction in water contact angle for bilayer films was observed for furcellaran/carboxymethyl cellulose-based films when lingonberry extract was incorporated into the furcellaran layer [40].

The evolution of the water contact angle as a function of time is presented in Figure 5b. The ambient atmosphere was not saturated with water vapor, and, as a consequence, the contact angle of the sessile droplet was expected to decrease with time. For the TPS/MCC sample, the contact angle decreased slowly, reaching  $87.6^\circ$  at the end of the analysis. A more pronounced decrease in contact angle was detected for the other samples, particularly for the samples with GA added at 10 mass% and 15 mass% contents (SM10 and SM15 samples). The higher absorption of the water droplet, observed for these bilayer samples, may be ascribed mainly to the hydrophilic character of GA, in which hydroxylic and carboxylic

acid groups are present. These results suggest that, for bilayer films, the surface contact angle for the first layer also depends on the composition of the second layer.

### 3.5. Oxygen Permeability

Oxidation is one of the processes that leads to the loss and waste of food products. Packaging can minimize this process by inhibiting the transfer of oxygen to the food. Table 1 shows the PV results, determined according to the literature [20,21] for canola oil, kept in containers covered with the prepared films. In the uncovered container (Control), canola oil has no protection against oxidation, leading to significantly higher ( $p < 0.05$ ) PV values. In contrast, the TPS/MCC film provides a barrier to oxygen gas. A significant decrease ( $p < 0.05$ ) in PV (PV =  $66.6 \pm 0.9$  meq/kg or  $0.85 \pm 0.01$  g/100 g) for the oil was observed. The TPS–MCC interaction contributes to a compact structure, and the MCC crystalline particles form a tortuous path to the diffusion of oxygen. By adding the electrospun layer (SM film), PV for the canola oil decreased significantly ( $p < 0.05$ ) to  $61.4 \pm 1.1$  meq/kg or  $0.78 \pm 0.01$  g/100 g. Besides the slight increase in thickness, the addition of EVOH, frequently used as an excellent oxygen barrier polymer, explains this result. In contrast, the incorporation of GA seems to exert no significant effect ( $p < 0.05$ ) on PV (Table 1), because the results pointed out a behavior similar to that of the SM film. The high antioxidant capacity of GA was expected to scavenge free radicals, which would improve PV and, consequently, the oxygen permeability, OP [41]. The much more probable degradation of GA at 60 °C for 7 days might be a plausible explanation for this result.

**Table 1.** Peroxide values (PV) for canola oil.

Sample <sup>A</sup>	PV * (meq/kg)	PV * (g/100 g)
Control	$71.2 \pm 1.4$ <sup>a</sup>	$0.9 \pm 0.02$ <sup>a</sup>
TPS/MCC	$66.6 \pm 0.9$ <sup>b</sup>	$0.85 \pm 0.01$ <sup>b</sup>
SM	$61.4 \pm 1.1$ <sup>c</sup>	$0.78 \pm 0.01$ <sup>c</sup>
SM5	$60.5 \pm 0.8$ <sup>c</sup>	$0.76 \pm 0.01$ <sup>c</sup>
SM10	$62.8 \pm 0.9$ <sup>c</sup>	$0.79 \pm 0.01$ <sup>c</sup>
SM15	$61.1 \pm 1.5$ <sup>c</sup>	$0.76 \pm 0.02$ <sup>c</sup>

<sup>A</sup> Control: Canola oil kept in an uncovered bottle; TPS/MCC: Canola oil covered with a film consisting of thermoplastic starch incorporated with microcrystalline cellulose; SM: Canola oil covered with a chitosan/poly(ethylene-co-vinyl alcohol) bilayer film produced without gallic acid; SM5, SM10 and SM15: Canola oil covered with bilayer films produced with 5%, 10% and 15% gallic acid, respectively. \* The results are given as the mean  $\pm$  standard deviation. Different superscript letters in a column indicate a significant difference among samples by the Tukey's test ( $p < 0.05$ ).

### 3.6. Mechanical Properties

Results from tensile tests performed for the thermoplastic starch composite (TPS/MCC) and for the bilayer films are shown in Figure 6 and Table S1. The low elongation at break determined for the TPS/MCC composite reflects the role of the added MCC, which reduces the extensibility of the material. Coating TPS/MCC with the electrospun CS/EVOH layer, with or without GA, caused no significant variation ( $p < 0.05$ ) in the mechanical properties of the bilayer films. However, observing the curves in Figure 6, a reduction in tensile strength and Young's modulus values is suggested for SM and SM5, compared with TPS/MCC. In contrast, the addition of GA at higher concentrations (SM10 and SM15) seems to have a positive effect on these properties. For these films, in relation to the bilayer film without GA (SM film), enhancements of 47% and 59% in tensile strength and 57% and 54% in Young's modulus were observed. This result may be associated with the formation of intermolecular hydrogen bonds between GA and the polymer components of the electrospun layer, as revealed by FTIR data. An increase in rigidity was also observed for glycerol-plasticized chitosan films, incorporated with GA at 10.0 and 20.0% contents [25]. These authors also attributed their results to the formation of physical interactions between GA and the polymer component.

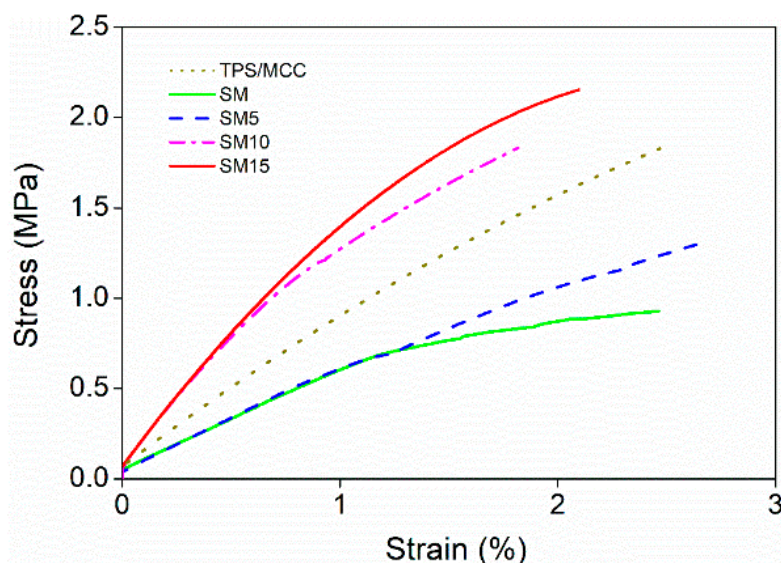


**Figure 6.** Stress versus strain curves from tensile tests obtained for the TPS/MCC composite and bilayer films formed by CS/EVOH/GA electrospun onto TPS/MCC with the addition of GA at 0% (SM), 5.0% (SM5), 10.0% (SM10), and 15.0% (SM15) concentrations. TPS: thermoplastic starch; MCC: microcrystalline cellulose; CS: chitosan; EVOH: poly(ethylene-co-vinyl alcohol); GA: gallic acid.

### 3.7. Antioxidant Activity

The antioxidant activity of the bilayer films was assessed by the DPPH free radical scavenging assay. The DPPH assay is often chosen to evaluate the hydrogen atom transfer (HAT) and the single electron transfer (SET) [42] or sequential proton loss electron transfer (SPLET) [43] capabilities of bioactive polyphenols (ArOH). DPPH is a crystalline powder. Its violet color in an ethanolic or methanolic solution is attributed to DPPH free radicals, which absorb at ~517 nm. In the presence of a sample with antioxidant properties, the violet color vanishes, leaving the solution colorless. DPPH interacts with phenolic compounds by the HAT mechanism by transferring the H atom of the hydroxylic group to DPPH directly. By the SET or SPLET mechanism, firstly, the ArOH compound is deprotonated, giving rise to a phenolic anion. Sequentially, the ArO<sup>-</sup> anion donates an electron to DPPH [43]. The incorporated GA was previously found to act as a potent antioxidant primarily by the HAT mechanism [42]. The high scavenging activity of GA (88.5%) against the DPPH radical is attributed to the three phenolic hydroxyl groups in its structure and the stabilization capacity of the resulting radical species by resonance [44]. Figure 7 and Table S2 show the results from the DPPH test, applied to the ethanolic solutions obtained by the extraction of the bilayer films. All films with the incorporation of GA presented antioxidant activity. For the film loaded with the lowest concentration of GA (SM5), extraction with 95% ethanol for 1 h led to a scavenging activity against the DPPH radical (RSA) of  $268.9 \pm 19.1 \mu\text{mol.L}^{-1}.\text{Eq.Trolox.g}^{-1}$ , or  $15.9 \pm 1.5\%$ . Even with an increase in GA content, over the first 3 h of extraction, no significant variation in RSA for the SM10 sample was observed in relation to the RSA value determined for SM5. As expected, the SM15 sample, with the highest content in GA, presented the highest RSA. Extraction for 24 h favored GA dissolution and release, and the RSA values increased with the amount of GA present in the ethanolic solution. Solubility and release conditions on RSA evaluations were also identified by other authors [45]. The antioxidant capacity reached  $903.8 \pm 62.2 \mu\text{mol.L}^{-1}.\text{Eq.Trolox.g}^{-1}$ , or  $(53.5 \pm 3.0)\%$  for the SM15 film, extracted for 24 h.

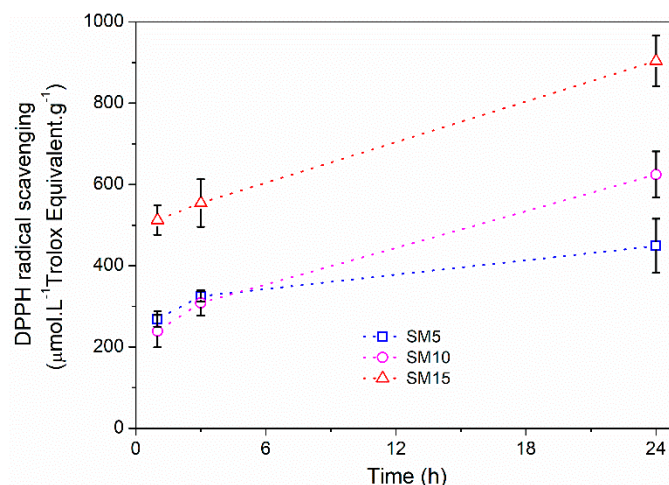


**Figure 7.** Free radical scavenging activity determined by the DPPH assay for the solutions extracted with aqueous ethanol at 95% for 1 h, 3 h, and 24 h from the CS/EVOH/GA films with the addition of GA at 5.0% (SM5), 10.0% (SM10), and 15.0% (SM15) concentrations, as a function of extraction time. TPS: thermoplastic starch; MCC: microcrystalline cellulose; CS: chitosan; EVOH: poly(ethylene-co-vinyl alcohol); GA: gallic acid.

#### 4. Conclusions

Antioxidant bilayer films were successfully prepared by incorporating gallic acid in nanofibers directly collected on a thermoplastic starch composite (TPS/MCC). The incorporation of MCC to TPS led to a water contact angle value of  $\theta_0 = 100.6^\circ$ , characteristic of hydrophobic surfaces. Increasing concentrations of hydrophilic GA led to increased wettability. Coating the TPS/MCC first layer with the CS/EVOH electrospun layer, with or without GA, allowed for improvement in oxygen permeability. The peroxide value determined for canola oil kept in containers covered with the films reached the lowest value of 60.5 meq/kg when covered with the SM5 bilayer film. A significant improvement in tensile strength, from 0.9 MPa (SM, bilayer film without GA) to 2.2 MPa (SM15, bilayer film with GA added at 15 mass % concentration), was observed. The solubility of GA in 95% ethanol seemed to compensate for the stability of the hydrogen bonding-formed network, leading to enhanced radical scavenging activities (RSA) as the GA concentration increased. The RSA varied from 512.5 to 903.8  $\mu\text{mol.L}^{-1}.\text{Eq. Trolox.g}^{-1}$  for the SM15 sample, after the 1 h and 24 h extractions, respectively. The bilayer films can be considered potential antioxidant films for application in the packaging of food products. Further experiments are still needed to fully characterize the bilayer films and evaluate their performance as packaging for model foods.

**Supplementary Materials:** The following supporting information can be downloaded at: <https://www.mdpi.com/article/10.3390/polysaccharides5020010/s1>, Figure S1: FTIR spectra for CS, EVOH and for the CS/EVOH electrospun film. Table S1: Thickness, stress at break ( $\sigma_{\text{max}}$ ), strain at break ( $\epsilon_{\text{max}}$ ) and Young's modulus (E) for the materials; Table S2: DPPH radical scavenging activity.

**Author Contributions:** R.F.G.: Conceptualization, Methodology, Formal analysis, Investigation, Validation, Visualization; Funding acquisition, Writing—original draft; C.T.A.: Conceptualization, Funding acquisition, Project administration, Resources, Supervision, Writing—review and editing. All authors have read and agreed to the published version of the manuscript.

**Funding:** This work was supported by the Conselho Nacional de Desenvolvimento Científico e Tecnológico (CNPq) [Grant n 306752/2022-0], Fundação Carlos Chagas Filho de Amparo à Pesquisa do Estado do Rio de Janeiro (FAPERJ) [Grant n E-26/010.000984/2019 Nanotechnology Network and E-26/205.796/2022], and Coordenação de Aperfeiçoamento de Pessoal de Nível Superior—Brasil (CAPES), Finance Code 001.

**Institutional Review Board Statement:** Not applicable.

**Data Availability Statement:** Data are contained within the article and Supplementary Materials.

**Conflicts of Interest:** The authors declare no conflict of interest.

## References

1. Numa, I.A.N.; Wolf, K.E.; Pastore, G.M. FoodTech startups: Technological solutions to achieve SDGs. *Food Humanit.* **2023**, *1*, 358–369. [[CrossRef](#)]
2. Zhao, Y.; Li, B.; Zhang, W.; Zhang, L.; Zhao, H.; Wang, S.; Huang, C. Recent advances in sustainable antimicrobial food packaging: Insights into release mechanisms, design strategies, and applications in the food industry. *J. Agric. Food Chem.* **2023**, *71*, 11806–11833. [[CrossRef](#)] [[PubMed](#)]
3. Lai, W.-F.; Wong, W.-T. Design and practical considerations for active polymeric films in food packaging. *Int. J. Mol. Sci.* **2022**, *23*, 6295. [[CrossRef](#)] [[PubMed](#)]
4. Kandemir, K.; Piskin, E.; Xiao, J.; Tomas, M.; Capanoglu, E. Fruit juice industry wastes as a source of bioactives. *J. Agric. Food Chem.* **2022**, *70*, 6805–6832. [[CrossRef](#)] [[PubMed](#)]
5. Aydogdu, A.; Sumnu, G.; Sahin, S. Fabrication of gallic acid loaded hydroxypropyl methylcellulose nanofibers by electrospinning technique as active packaging material. *Carbohydr. Polym.* **2019**, *208*, 241–250. [[CrossRef](#)] [[PubMed](#)]
6. Fang, Z.; Bhandari, B. Encapsulation of polyphenols—A review. *Trends Food Sci. Technol.* **2010**, *21*, 510–523. [[CrossRef](#)]
7. Avossa, J.; Herwig, G.; Toncelli, C.; Itel, F.; Rossi, R.M. Recent advances in electrospinning of nanofibers from bio-based carbohydrate polymers and their applications. *Trends Food Sci. Technol.* **2022**, *120*, 308–324. [[CrossRef](#)]
8. Hosseini, S.F.; Gómez-Guillén, M.C. A state-of-the-art review on the elaboration of fish gelatin as bioactive packaging: Special emphasis on nanotechnology-based approaches. *Trends Food Sci. Technol.* **2018**, *79*, 125–135. [[CrossRef](#)]
9. Wen, P.; Zhu, D.-H.; Wu, H.; Zong, M.-H.; Jing, Y.-R.; Han, S.-Y. Encapsulation of cinnamon essential oil in electrospun nanofibrous film for active food packaging. *Food Control* **2016**, *59*, 366–376. [[CrossRef](#)]
10. Zhang, Y.; Min, T.; Zhao, Y.; Cheng, C.; Yin, H.; Yue, J. The developments and trends of electrospinning active food packaging: A review and bibliometrics analysis. *Food Control* **2024**, *160*, 110291. [[CrossRef](#)]
11. Díaz-Montes, E. Polysaccharide-based biodegradable films: An alternative in food packaging. *Polysaccharides* **2022**, *3*, 761–775. [[CrossRef](#)]
12. Popyrina, T.N.; Demina, T.S.; Akopova, T.A. Polysaccharide-based films: From packaging materials to functional food. *J. Food Sci. Technol.* **2022**, *60*, 2736–2747. [[CrossRef](#)] [[PubMed](#)]
13. Siddiqui, S.A.; Yang, X.; Deshmukh, R.K.; Gaikwad, K.K.; Bahmid, N.A.; Castro-Muñoz, R. Recent advances in reinforced bioplastics for food packaging—A critical review. *Int. J. Biol. Macromol.* **2024**, *263*, 130399. [[CrossRef](#)]
14. Wang, Q.; Chen, W.; Zhu, W.; McClements, D.J.; Liu, X.; Liu, F. A review of multilayer and composite films and coatings for active biodegradable packaging. *NPJ Sci. Food* **2022**, *6*, 18. [[CrossRef](#)]
15. Grzebieniarsz, W.; Biswas, D.; Roy, S.; Jamróz, E. Advances in biopolymer-based multi-layer film preparations and food packaging applications. *Food Packag. Shelf Life* **2023**, *35*, 101033. [[CrossRef](#)]
16. Kalantari, K.; Afifi, A.M.; Jahangirian, H.; Webster, T.J. Biomedical applications of chitosan electrospun nanofibers as a green polymer—Review. *Carbohydr. Polym.* **2019**, *207*, 588–600. [[CrossRef](#)]
17. Marangoni Júnior, L.; Oliveira, L.M.; Bócoli, P.F.J.; Cristianini, M.; Padula, M.; Anjos, C.A.R. Morphological, thermal and mechanical properties of polyamide and ethylene vinyl alcohol multilayer flexible packaging after high-pressure processing. *J. Food Eng.* **2020**, *276*, 109913. [[CrossRef](#)]
18. Gouvêa, R.F.; Ferreira, W.H.; Souto, L.F.C.; Gonçalves, R.P.; Soares, B.G.; Andrade, C.T. Flexible dielectric ZnO-doped reduced graphene oxide bionanocomposites from solution blending for potential application in bio-related devices. *J. Appl. Polym. Sci.* **2021**, *138*, e51186. [[CrossRef](#)]
19. Kenawy, E.-R.; Layman, J.M.; Watkins, J.R.; Bowlin, G.L.; Matthews, J.A.; Simpson, D.G.; Wnek, G.E. Electrospinning of poly(ethylene-co-vinyl alcohol) fibers. *Biomaterials* **2003**, *24*, 907–913. [[CrossRef](#)]
20. Kurt, A.; Kahyaoglu, T. Characterization of a new biodegradable edible film made from salep Glucomannan. *Carbohydr. Polym.* **2014**, *104*, 50–58. [[CrossRef](#)]
21. Zhou, Y.; Wu, X.; Chen, J.; He, J. Effects of cinnamon essential oil on the physical, mechanical, structural and thermal properties of cassava starch-based edible films. *Int. J. Biol. Macromol.* **2021**, *184*, 574–583. [[CrossRef](#)] [[PubMed](#)]
22. Jiang, Y.; Zhao, G.; Yang, X.; Fan, F. Preparation and characterization of nano-SiO<sub>2</sub>-modified emulsified film and its application for strawberry preservation. *Food Packag. Shelf Life* **2023**, *40*, 101181. [[CrossRef](#)]
23. ISO 527-3:2018; Plastics—Determination of Tensile Properties—Part 3 Test Conditions for Films and Sheets. International Organization for Standardization, ISO Central Secretariat: Geneva, Switzerland, 2018.
24. Chollakup, R.; Pongburoos, S.; Boonsong, W.; Khanoonkon, N.; Kongsin, K.; Sothornvit, R.; Sukyai, P.; Sukatta, U.; Harnkarnsujarit, N. Antioxidant and antibacterial activities of cassava starch and whey protein blend films containing rambutan peel extract and cinnamon oil for active packaging. *LWT-Food Sci. Technol.* **2020**, *130*, 109573. [[CrossRef](#)]
25. Zarandona, I.; Puertas, A.I.; Duñas, M.T.; Guerrero, P.; dela Caba, K. Assessment of active films incorporated with gallic acid. *Food Hydrocoll.* **2020**, *101*, 105486. [[CrossRef](#)]

26. Wang, P.; Wang, H.; Liu, J.; Wang, P.; Jiang, S.; Li, X.; Jiang, S. Montmorillonite@chitosan-poly (ethylene oxide) nanofibrous membrane enhancing poly (vinyl alcohol-co-ethylene) composite film. *Carbohydr. Polym.* **2018**, *181*, 885–892. [[CrossRef](#)]
27. Arkoun, M.; Daigle, F.; Holley, R.A.; Heuzey, M.C.; Aji, A. Chitosan-based nanofibers as bioactive meat packaging materials. *Packag. Technol. Sci.* **2018**, *31*, 185–195. [[CrossRef](#)]
28. Panda, P.K.; Park, K.; Seo, J. Development of poly(vinylalcohol)/regenerated chitosan blend film with superior barrier, antioxidant, and antibacterial properties. *Progr. Org. Coat.* **2023**, *183*, 107749. [[CrossRef](#)]
29. Zakani, B.; Grecov, D. Effect of ultrasonic treatment on yield stress of highly concentrated cellulose nano-crystalline (CNC) aqueous suspensions. *Carbohydr. Polym.* **2022**, *291*, 119651. [[CrossRef](#)] [[PubMed](#)]
30. Günzler, H.; Böck, H. *IR-Spektroskopie Eine Einführung*, 1st ed.; Verlag Chemie: Weinheim, Germany, 1975; pp. 206–211.
31. Li, T.; Liu, R.; Zhang, C.; Meng, F.; Wang, L. Developing a green film from locust bean gum/carboxycellulose nanocrystal for fruit preservation. *Future Foods* **2021**, *4*, 100072. [[CrossRef](#)]
32. Liu, Y.; Wang, J.; Yue, H.; Du, Z.; Cheng, X.; Wang, H.; Cheng, F.; Du, X. Flame-retardant phytic acid-decorated thermoplastic starch/halloysite nanotube composite films with enhanced mechanical strength and excellent barrier properties. *Carbohydr. Polym.* **2024**, *323*, 121465. [[CrossRef](#)]
33. Ferreira, W.H.; Carmo, M.M.I.B.; Silva, A.L.N.; Andrade, C.T. Effect of structure and viscosity of the components on some properties of starch-rich hybrid blends. *Carbohydr. Polym.* **2015**, *117*, 988–995. [[CrossRef](#)]
34. Almeida, T.; Karamysheva, A.; Valente, B.F.A.; Silva, J.M.; Braz, M.; Almeida, A.; Silvestre, A.J.D.; Vilela, C.; Freire, C.S.R. Biobased ternary films of thermoplastic starch, bacterial nanocellulose and gallic acid for active food packaging. *Food Hydrocoll.* **2023**, *144*, 108934. [[CrossRef](#)]
35. Chen, N.; Gao, H.-X.; He, Q.; Yu, Z.-L.; Zeng, W.-C. Interaction and action mechanism of starch with different phenolic compounds. *Int. J. Food Nutr.* **2020**, *71*, 726–737. [[CrossRef](#)] [[PubMed](#)]
36. Law, K.-L. Definitions for hydrophilicity, hydrophobicity, and superhydrophobicity: Getting the basics right. *J. Phys. Chem. Lett.* **2014**, *5*, 686–688. [[CrossRef](#)]
37. Ahmad, D.; van den Boogaert, I.; Miller, J.; Presswell, R.; Jouhara, H. Hydrophilic and hydrophobic materials and their applications. *Energ. Sources Part A* **2018**, *40*, 2686–2725. [[CrossRef](#)]
38. Magalhães, N.F.; Andrade, C.T. Thermoplastic corn starch/clay hybrids: Effect of clay type and content on physical Properties. *Carbohydr. Polym.* **2009**, *75*, 712–718. [[CrossRef](#)]
39. Debnath, B.; Duarah, P.; Haldar, D.; Purkait, M.K. Improving the properties of corn starch films for application as packaging material via reinforcement with microcrystalline cellulose synthesized from elephant grass. *Food Packag. Shelf Life* **2022**, *34*, 100937. [[CrossRef](#)]
40. Jamróz, E.; Tkaczewska, J.; Juszcak, L.; Zimowska, M.; Kawecka, A.; Krzysciak, P.; Skóra, M. The influence of lingonberry extract on the properties of novel, double-layered biopolymer films based on furcellaran, CMC and a gelatin hydrolysate. *Food Hydrocoll.* **2022**, *124*, 107334. [[CrossRef](#)]
41. Zhang, N.; Li, Y.; Wen, S.; Sun, Y.; Chen, J.; Gao, Y.; Sagymbek, A.; Yu, X. Analytical methods for determining the peroxide value of edible oils: A mini-review. *Food Chem.* **2021**, *358*, 129834. [[CrossRef](#)]
42. Leopoldini, M.; Marino, T.; Russo, N.; Toscano, M. Antioxidant properties of phenolic compounds: H-Atom versus electron transfer mechanism. *J. Phys. Chem. A* **2004**, *108*, 4916–4922. [[CrossRef](#)]
43. Liu, Z.-Q. Chemical methods to evaluate antioxidant ability. *Chem. Rev.* **2010**, *110*, 5675–5691. [[CrossRef](#)] [[PubMed](#)]
44. Mathew, S.; Abraham, T.E.; Zakaria, Z.A. Reactivity of phenolic compounds towards free radicals under in vitro conditions. *J. Food Sci. Technol.* **2015**, *52*, 5790–5798. [[CrossRef](#)] [[PubMed](#)]
45. Rao, Z.; Lei, X.; Chen, Y.; Ling, J.; Zhao, J.; Ming, J. Facile fabrication of robust bilayer film loaded with chitosan active microspheres for potential multifunctional food packing. *Int. J. Biol. Macromol.* **2023**, *231*, 123362. [[CrossRef](#)] [[PubMed](#)]

**Disclaimer/Publisher’s Note:** The statements, opinions and data contained in all publications are solely those of the individual author(s) and contributor(s) and not of MDPI and/or the editor(s). MDPI and/or the editor(s) disclaim responsibility for any injury to people or property resulting from any ideas, methods, instructions or products referred to in the content.